Passive Capacitive based Approach for Full Body Gym Workout Recognition and Counting

Sizhen Bian
German Research Center for Artificial Intelligence
Kaiserslautern, Germany
sizhen.bian@dfki.de

Vitor F Rey
German Research Center for Artificial Intelligence
Kaiserslautern, Germany
vitor.fortes@dfki.de

Peter Hevesi
German Research Center for Artificial Intelligence
Kaiserslautern, Germany
peter.hevesi@dfki.de

Paul Lukowicz
German Research Center for Artificial Intelligence
Kaiserslautern, Germany
paul.lukowicz@dfki.de

***Abstract*—In this work, we present the design and implementation of a micro watt level power consumption, human body capacitance based sensor for recognizing and counting gym workouts. The concept also works when the device is attached to a body part which is not directly involved in the activity's movement. In contrast, most of the widely used motion sensing based approaches require placing the sensor on the moving body part (e.g. for analyzing leg based gym exercises the sensor needs to be placed on the leg). We described the physical principle behind the ubiquitous electric coupling between human body and environment, and explored the capability of this sensing modality in gym workouts. We evaluated our sensor with 11 subjects, performing 7 popular gym workouts each day over 5 days with our sensor being placed at 3 different body positions, including a non-contact position, where the sensor is placed in the subject's pocket. Results showed that our sensing approach achieved an average counting accuracy of 91%, which is highly competitive with commercial devices on the market. The mean leave one user out workout recognition f-scores obtained were of 63%, 56%, 45% for sensors located on wrist, on calf and in pocket, respectively. As every subject performed activities over multiple days changing shoe height, shoe and clothes type, we demonstrate that full body activity counting and to some extent recognition is feasible, regardless of personal habit of movement speed and scale.**

***Index Terms*—human body capacitance, activity recognition, counting**

I. Introduction

Going to the gym is an important part of a healthy lifestyle for many people. As a consequence, plenty of computer-aided fitness monitors were developed to help users record, analyze and improve their workout quality. Moreover, body sensing and activity recognition is a key topic in pervasive computing, essential in a broad range of applications including ambient assisted living.

Conventionally, gym monitors mainly rely on digital consumer devices [1]. For example, Mitchell [2] presented a framework that allows automatic identification of sport activities with smartphone accelerometers. Fu et al. [3] proposed a novel approach with speaker and microphone that are integrated into a smartphone to track fitness exercises performed close to it. Those digital device based approaches for activity recognition have their limitations, being constrained to a narrow set of activities. For example, an accelerometer in the leg will not be able to sense arm movement.

Another possible approach, which is influenced by whole body motion, is to use capacitance sensors to monitor gym activities. The human body, insulated from ground, is a conductor with a certain capacitance and resistance (with respect to ground). A series of experiments from Jonassen et al. [4] and Fujiwara et al. [5] gave *Human Body Capacitance*(HBC) a value of 100-400 *p*f. Plenty of *HBC* based sensors and applications were developed: proximity sensing [6], movement detection [7], communication [8]–[10] and motion recognition [11]. Most of those works basically use active sensors with capacitance changing in shunt mode or transmit mode, which use a transceiver to emit and capture a time-varying signal.

In contrast, in a passive sensing approach with capacitance changing in loading mode, the sensing instrument can be significantly simplified, thus improving the power consumption. Considerable work has been done recently to optimize the availability, portability as well as power consumption of *HBC* based passive sensors and applications. Cohn et al. [12] developed an wearable ultra-low-power capacitance based human body motion sensor, as well as Pouryazdan et al. [13], sensing hair touch and leg movement. Wilmsdorff at al. [14] expand this purely passive capacitive measurement technique with a wide range of applications in interior spaces and outdoors. Sensing hardware has also been explored [15], [16]. The most important advantage of these works is the low power consumption. Our research also related to the field of passive electric field sensing. However we focused on a simpler sensing circuit as well as on a study in gym workout recognition and counting to show the wide range of application possibilities using this technology.

In this paper we present a *HBC* based capacitive coupling sensor for full body gym workout recognition and counting, aiming to provide an alternative to gym workout monitors. With a simple sensing hardware, which is composed of discrete components, the change of the coupling strength between body and environment can be perceived by sensing

978-1-5386-9148-9/19/$31.00 ©2019 IEEE

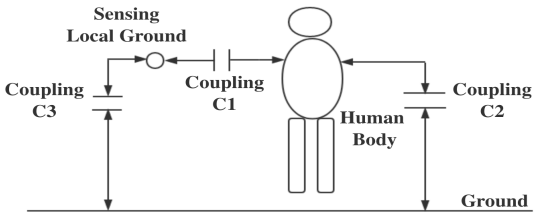

Fig. 1: Capacitive Coupling among Body, Environment and sensing local Ground

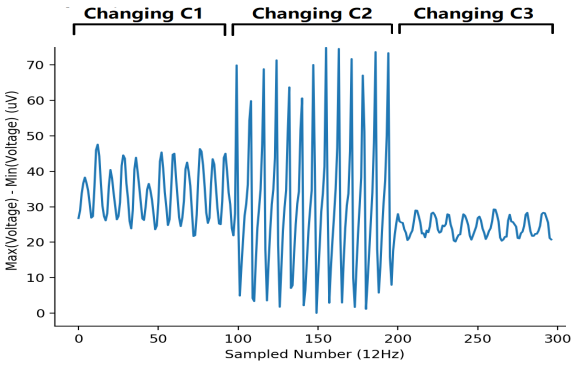

(a) Charge Redistribution caused Voltage Variation

(b) Changing C1 (Distance: 1.1cm - 2.8cm)

(c) Changing C2 (Distance: 1.5cm - 10.0cm)

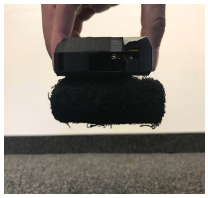

(d) Changing C3 (Distance: 2.8cm - 5.8cm)

Fig. 2: Charge redistribution caused voltage variation when changing the three involved coupled capacitors

the local potential change on the body. Movement of human body will cause charge redistribution on the body included sensing circuit, the quantity and frequency of charge change is related to lots of factors, like moving speed and scale, subject's wearing. To verify the feasibility of our sensor, a study of gym workout recognition and counting was carried out. We recorded 11 subjects performing 7 widely trained gym activities with sensors in 3 different body locations: on the calf, wrist and inside the subject's pocket. Results present a high accuracy with counting and acceptable performance in recognition, demonstrating that full body gym activity counting and to some extent recognition with capacitive coupling based approach is feasible. Overall, in this paper we present the following contributions:

1) We developed a more simple sensing circuit for *HBC* based motion sensing, which has power consumption on the μV level, being the simplest among related work that is able to sense *HBC* based body movement.
2) We evaluated our system with 11 subjects in a study involving 7 types of gym workouts with our sensors placed on wrist, calf and inside subject's pocket, obtaining a leave one user out f-measure of 63%, 56%, 45% in activity recognition respectively. For counting we achieved an average accuracy of 91%, which is competitive with existing wearable digital devices [17]. Users performed workouts over multiple days with different clothing, footwear, weather conditions as well as individual preference of moving speed and scale, demonstrating the robustness of our system.

II. Physical Background and Sensing Prototype

Our sensing approach relies on *HBC* based coupling between body and environment ground(C2 in Fig. 1). As a conductor, the human body acts as one plate of the coupled capacitor, while the environment, mainly the ground, acts as another plate [18]. Because of the triboelectric effect [19] and other environmental electric sources nearly all our surrounding objects carry a certain amount of charge. Assuming that the charge on a human body is Q_B and the instantaneous capacitance between body and ground is C_B, then the potential of the body U_B can be expressed as:

$$U_B = \frac{Q_B}{C_B} \tag{1}$$

The potential on the body is not constant, it will change along with the change of on-body charge and body-ground capacitance. For example, the triboelectric effect between skin and wearing affects Q_B, while the relative body movement affects C_B:

$$\frac{d}{d_t}(U_B(t)) = \frac{d(Q_B(t))}{d_t} / \frac{d(C_B(t))}{d_t} \tag{2}$$

$$\frac{d(C_B(t))}{d_t} = \varepsilon_0 \varepsilon_r \frac{d(A(t))}{d(D(t))} \tag{3}$$

where ε_0 is the vacuum permittivity, ε_r is the relative permittivity, A and D is the square of overlapping area and distance between human body and ground, respectively. Capacitance will change with the variation of relative distance or overlapping area of the capacitor, which will cause a quick charge flow at the sensing hardware. Thus, by sensing the voltage variation of the body, which is caused by patterns of capacitance change, we can derive the relative movement of our body.

Besides the coupling between body and ground, there are two other couplings involved, namely the one between local ground(the ground of sensing circuit) and body (C1 in Fig. 1), and another one between local ground and environmental ground (C3 in Fig. 1). Thus the capacitance from sensing

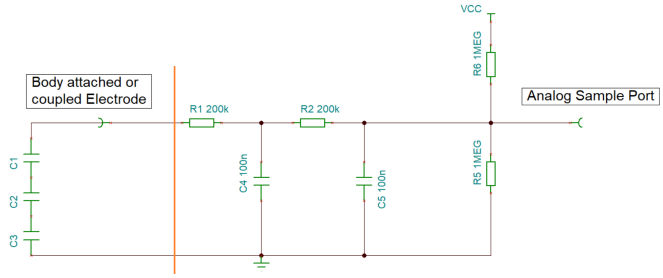

Fig. 3: Analog Front End(right part)

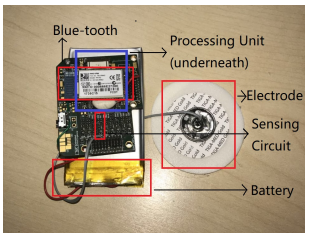

Fig. 4: Hardware including sensing, processing, wireless transmission and battery units

Fig. 5: Hardware attached to Wrist

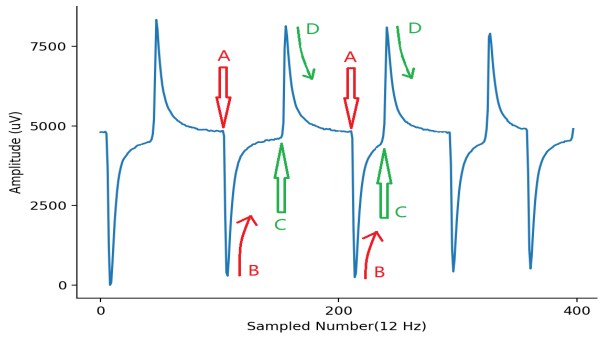

Fig. 6: Potential change process of leg lift(A) and drop(C) (Distance of feet to ground: 2.5-20cm) with sensor on a table and electrode attached to body. Arrow A is the point of lifting leg, Arrow C is the point of dropping leg. Arrow B and D indicate the process of charge redistribution

electrode(a small conductive plate from sensing hardware, see Fig. 4) to local ground is:

$$C_c = C_1 + C_2 + C_3 \tag{4}$$

The variation of capacitance from each coupling will affect the voltage variation of local electrode. Fig. 2 shows the sensed body potential variation when the capacitance of each coupling is changed repetitively. C1 is changed by enlarging and diminishing the distance between body surface and local ground of sensing hardware. C2 is changed by lifting the leg slightly while wearing the sensor on the wrist. C3 is changed by lifting the sensor away from and close to the environmental ground. The result of this three movements also reflect 2, where capacitance change will obviously contribute to potential variation U_B.

In our sensing front end design (see Fig. 3), we only use a simple voltage divider composed of two high value resistors and a second order passive low pass filter, which consumes only several μW power, less than active filter based sensing front ends([12]–[14], [20]). Assuming there is no filter, the sensed voltage could be described as:

$$V_s = V_{cc}\frac{Z_{(R_5)\|(C_1+C_2+C_3)}}{R_5+R_6} \tag{5}$$

$$Z_{(R_5)\|(C_1+C_2+C_3)} = \frac{R_5 j\omega C_c}{R_5 + j\omega C_c} \tag{6}$$

where ω is the angular frequency. R_5 has the same value of R_6, and combining the above two equations, the relation between V_{cc} and V_s is:

$$\frac{V_{cc}}{V_s} = 2 + \frac{R_5}{j\omega C_c} \tag{7}$$

Equation 7 shows that the repetitive change of capacitance will lead to a repetitive voltage variation. Besides that, the value of R_5 also plays a role in sensing sensitivity, a higher value contributing to a higher sensitivity. In our case here we use $1M$ ohm resistors. By adding the passive second order low pass filter, the impedance of the analog sensing part is not only composed of C_c. If Z_a is the new impedance, then:

$$\frac{V_{cc}}{V_s} = 2 + R_5 Z_a \tag{8}$$

$$Z_a = (((R_1 + C_c)\|C_4) + R_2)\|C_5 \tag{9}$$

Here we use same value of C_4 and C_5, as well as R_1 and R_2(Fig. 3), so we use R and C to replace them. Combining the two previous equations we have:

$$\frac{V_{cc}}{V_s} = 2 + R_5\frac{j\omega CC_c + 2C_cR + CR}{j^2\omega^2C^2C_c^2R + j\omega(2CC_cR + C^2R + CC_c) + C_c + C} \tag{10}$$

Equation 10 describes the whole analog sensing circuit. The passive second order low pass filter with a cut-off frequency of 7.96 Hz filters noise from the environment. Besides that, the filter contributes significantly to the charge redistribution when C_c changes. Equation 10 implies that a lower value of C will increase the response time. Here we designed the filter with a time constant of 20 ms. After each movement, for example, lifting a leg, the potential of the body will change, but this change will be immediately balanced by the process of charge redistribution, namely charging and discharging, until the potential of the electrode returns back to its former value. This balanced potential is decided by the sensing circuit, as Fig. 3 showed. From 3 it is clear, when the leg is lifted, that the capacitance(C_c) will drop immediately, and thus the potential will decrease correspondingly(as in 10, with C_c at the power of one at the numerator, and two at the denominator). To balance the charge distribution, the extra charge on C_c will then complement the voltage decrease at the analog sample port(Fig. 3), which is described as charging, depicted as arrow B in Fig. 6. The opposite process will explain the potential change process at arrow C and D.

Comparing the amplitude of leg lift and drop from Fig. 2a(middle: changing C2) and Fig. 6, where the subject had the

same wearing and the action took place at the same spot(same floor), the only two changed parameters are the position of the sensor and the action scale(distance of feet to ground). We believe that in this experiment the significant amplitude difference is mainly due to the sensor position. Equation 10 explains this difference, as when the sensor is placed on the table, the coupling strength($C1$) is significantly decreased, making the sensed potential variation much bigger than that when sensor is very close to the body.

For data sampling we use a 24 bits analog-digital converter ADS 1294 from Texas Instruments and wireless Bluetooth transmitter RN42 from Microchip Technology (Fig. 4). A simple wearable prototype depicted in Fig. 5 was built.

III. Experiment Setup

To evaluate our sensor, 7 widely trained workouts were selected, namely: Leg Curl, Leg Press, Squat, Abductor, Bench Press, Walking and Running. According to personal preference and habit, the previous five workouts were done with help of fitness equipment(except Squat) at a frequency between 0.8Hz and 1.8 Hz on a gym floor which is mainly made of concrete. Running is performed on treadmills, the surface of which is made of plastic, with a speed between 7km/h and 8km/h. Walking is composed of two states, one is walking on treadmills with a speed between 4.0km/h and 5.5km/h, another one is the random walking on the gym floor when the subjects move from one fitness equipment to another, in this state the speed is uncontrolled.

A total number of 11 subjects, labeled from A to K, including 4 female and 7 male, performed those 7 workouts. All of them are students with weight from 51kg to 80kg and height from 156cm to 189cm. 6 of them go to the gym at least 3 times a week, 5 of them are novices. Each subject performed all 7 workouts five times within 5 different days. During the exercises, data was transmitted from the sensors to a laptop via Bluetooth. All electrode potential readings were saved, and workout sessions were labelled in real time using a simple graphical user interface on the laptop. On each day every workout was done for 3 consecutive times, each time containing around 10 repetitions(for Walking and running on a treadmill, each time contains from 30 to 60 steps, step numbers are also recorded). All together, we got 5 sessions of whole day workouts for each subject with each sensor position: on wrist, on calf and in pocket. Within each session there are 3 segments of each workout. Regardless of subjects, we got 165 segments of each workouts with each sensor position.

During the 5 days' exercise, the temperature ranged from 15.9 °C to 28.4 °C, relative humidity ranged from 29% to 95%(Data is from WetterKontor GmbH, measured by HMP45D). The wearing of subjects was configured by three variations: height of shoe sole, shoe sole material (PVC or rubber), clothes material (polyester or cotton, as those materials are the most common materials in sport garments). Table I shows the configuration of the 11 participants' wearing configuration. As explored by Jonassen [4], it is hard to know which factors govern the variation of body capacitance. Because of the triboelectric effect [19] we believe that variations in wearing will influence the performance of our sensor. Thus we collected data with different configurations to validate recognition and counting in different scenarios and in future work to evaluate the influence of those on the signal.

As declared, our sensor will be placed at three positions on each person: on wrist, on calf and in pocket. With the first two placements the electrode will be attached to the skin. With the human body being used as part of the measuring electrode, the potential change of the body will be easily perceived. Those on-body tests will verify the functionality of full body motion monitoring by our sensor. When placing our sensor in the pocket, the electrode is loosely coupled with the body, and so we believe the potential change from the body will also cause charge redistribution at the electrode's side, though not so clear as in the attached deployments. The portability of this setup is also a huge advantage and thus it is interesting to test if our sensor is feasible with this off body placement.

TABLE I
Participants' Configuration Across Days

	First Day	Second Day	Third Day	Fourth Day	Fifth Day
Clothes Material	polyester	polyester	cotton	polyester	polyester
shoe sole height[a]	M	M	M	S	M
shoe sole material	PVC	PVC	PVC	PVC	rubber

[a] For each user, M and S denote the height of shoe sole, with M meaning the height of the pair of shoes the user is used to wear, while S denotes the different height of another shoe belonging to the subject. Different users had different shoe heights of M and S.

IV. Exploration of Capabilities

Most workouts will generate regular and repetitive signals, utilizing their statistical characteristics, like amplitude, frequency etc, workout classification and counting can be explored.

Fig. 7 shows the sensed activity signals from subjects C and E with three sensor locations. The repetitive peaks in every figure come from the repetitive body motions. Some of the activities generate multiple peaks each time, for example, in the signal from Leg Press when the sensor is attached to C's wrist, one of the reasons could be that, when a movement happens, not only the coupling strength between body and ground changes (C2 in Fig. 1), but also the one between the sensor's local ground and environmental ground(C3 in Fig. 1) changes. Another possible reason comes from the charge variation of the body caused by friction between skin and clothes. Some exceptions are Bench Press when the sensor is in the pocket, where it is hard to capture the peak visually. In this case, the body movement range is much smaller than other activities, and thus the potential change is so small that the sensor can hardly perceive it. But this didn't apply to all participants, as signal from some of them when doing Bench Press with the sensor in the pocket also generated potential

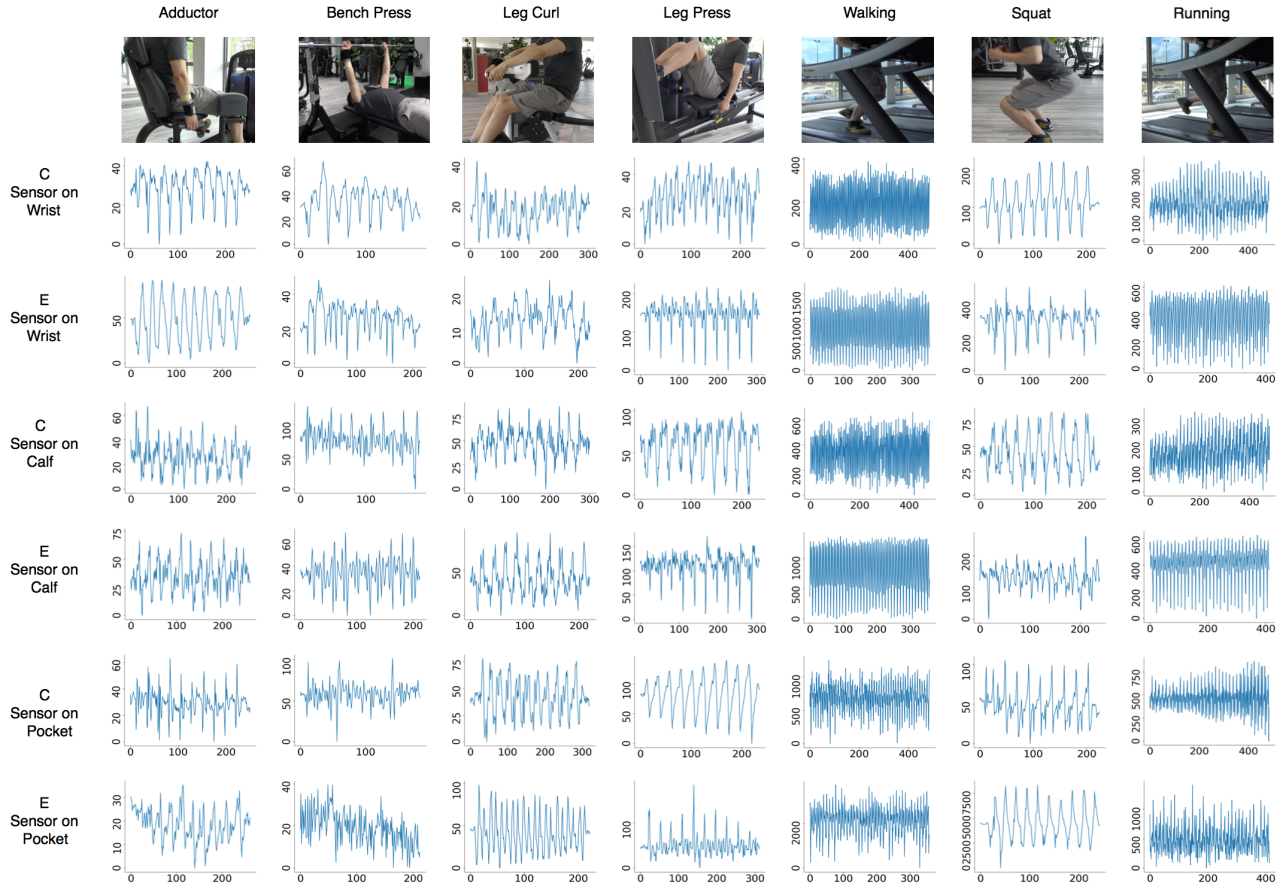

Fig. 7: Potential variation of 7 workouts from Participants C and E at first day with sensor at different positions (X axis: Sampled Number(12 Hz), Y axis: Voltage Scale(μV))

variation caused by the regular motion. We believe this is influenced by personal style of moving speed when performing Bench Press, as we declared, the individual moving speed also affect the potential variation at electrode side, which is also a reason for the uncertainty of those signals. An example is showed in Fig. 7, where C and E are doing Leg Press with sensor on the wrist with highly different scale of potential variation.

As discussed above, there is plenty of uncertain factors that will influence the body capacitance based movement exploration. In this work we try to use in some degree the patterns present in the workouts with our capacitance-based sensor, in order to recognize and count workouts regardless of personal mannerisms, wearing as well as weather conditions.

V. Gym workout classification

First, since the capacitance value varies according to many factors, and in fact the value of capacitance for each human body is not identical [21], we will use as features for classification changes in capacitance in μV instead of their raw μV values. The maximum absolute change allowed is $3mV$ and any bigger change is considered as an outlier and replaced by either $3mV$ or $-3mV$, according to its direction. As the sensor sampling rate is 12 Hz, the data is then subjected to a linear interpolation so that every second will have 24 readings.

Instances are generated using a sliding window approach where a window of 4 seconds (96 readings) is employed with a 1 second step. Windows are generated for each day and include moments where the subject is not performing any of the selected workout classes. Those moments are regarded as belonging to a new class named ”still”. Any time between repetitions is considered part of this class, except when the user is walking across the gym which is considered an instance of the ”Walking” class for recognition purposes only, as steps were not counted in those cases.

A. Network Architecture

As a classifier we employed a residual deep convolutional neural network that uses dilated convolutions, similar to *TCN* [22]. This architecture was selected as it was successful in many sequence modeling tasks, outperforming even LSTMs [22]. Notice that all convolutions in this architecture use *same* padding, which is convenient for going deeper as in our case each instance consists of a one-dimensional vector with window size (96) values.

The full network architecture can be seen in Fig. 8, and was implemented using keras [23] with the tensorflow [24]

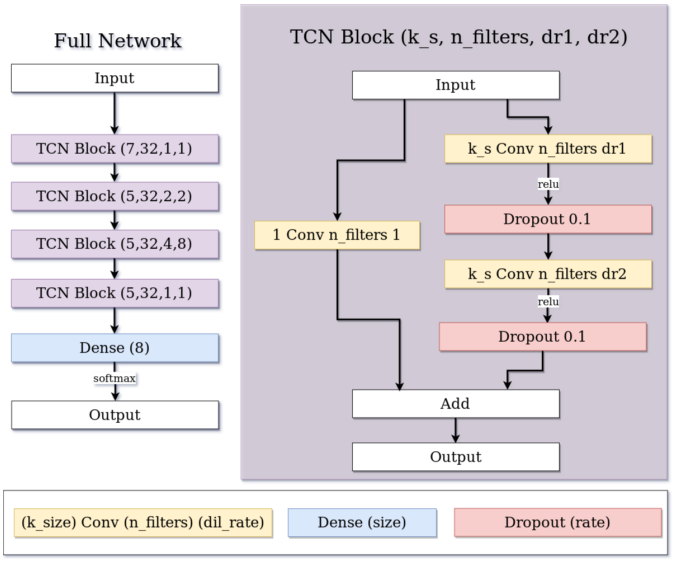

Fig. 8: Architecture for the neural network used for classification

backend. It was trained using the categorical cross-entropy loss function and the Adam optimizer [25] with 0.001 learning rate and 0.9 and 0.999 for β_1 and β_2, respectively. Since the dataset is highly imbalanced, containing more "still" instances than any other exercise, every training instance is weighted based on the labels present inside the window. The total weight of a window is inversely proportional to the frequency of its labels in the dataset and is calculated based on the labels of a window W as

$$\sum_{wi}^{W} \frac{N}{count(cl_{wi})}$$

where N represents the summed total number of timesteps in all training windows, $count(cl_i)$ represents the number of those timesteps that belong to class cl_i and cl_{wi} is the class label at timestep wi.

Each model is trained for 500 epochs with early stopping using a patience of 15 to avoid overfitting. The evaluation set used for the early stopping procedure consists of a random sample of the training set, with 20% of its instances.

B. Classification Results

In order to show that we can learn to recognize activities across subjects, we employed a **leave one user out** procedure where, for each fold, the test set contains all days of one subject, while the training set contains all days for the remaining ones. For activity recognition, we evaluated our model generating test labels in different modalities:

- One label per workout, where its prediction is generated by majority voting of its sliding window labels.
- One label per sliding window determined by majority voting inside the window.

The results for all those modalities can be seen in II. We show in Fig. 9 the joined confusion matrices for the one label per workout modality while the joined confusion matrices for one label per window can be seen in Fig. 10. In general,

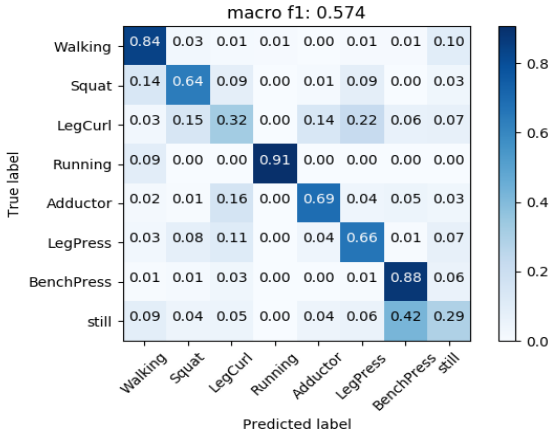

(a) Sensor on subject's Calf

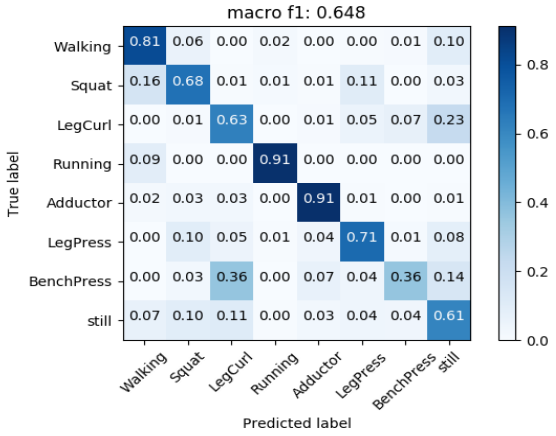

(b) Sensor on subject's Wrist

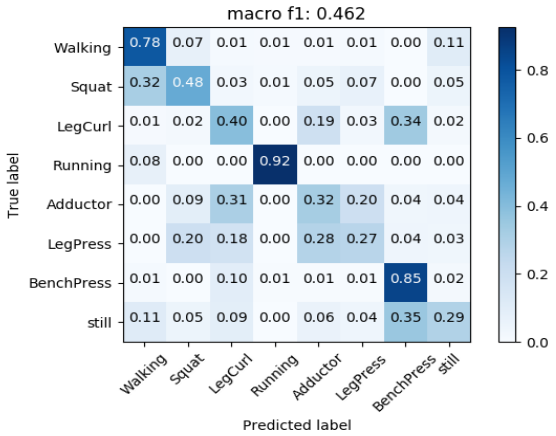

(c) Sensor on subject's Pocket

Fig. 9: All combined confusion matrices for one label per session.

classification of the Walking and Running activities worked in all sensor positions, including the sensor position in pocket, with a classification of over 80%. For workouts of Squat, Leg Curl, Leg Press and Adductor, the recognition accuracies are over 50% when sensor is on wrist and calf, except that Leg Curl with sensor on calf was highly classified as the other three

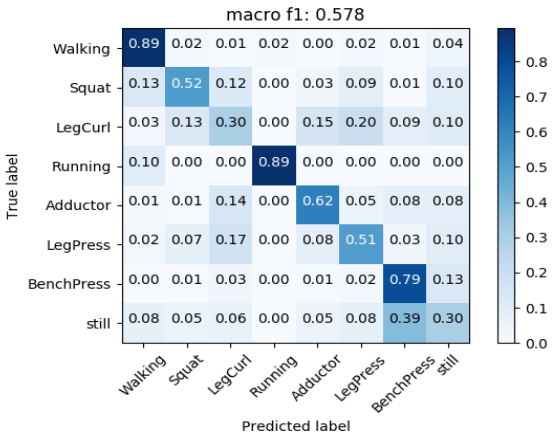

(a) Sensor on subject's Calf

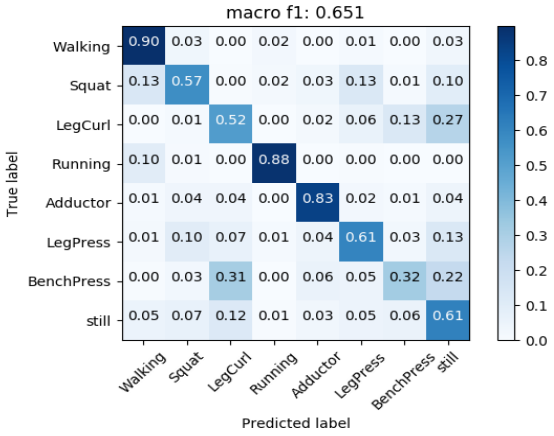

(b) Sensor on subject's Wrist

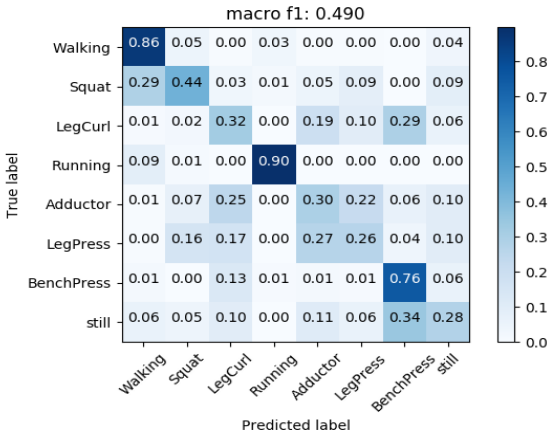

(c) Sensor on subject's Pocket

Fig. 10: All combined confusion matrices for one label per window.

workouts. Within those four workouts, Adductor's recognition accuracy with sensor on wrist shows the best with almost 90%. To be noticed is that the high level of misclassification from Squat to Walking across sensor positions. The possible reason is that the random walking between exercises sometimes generates a similar potential variation signal to Squats, which is different from the regular walking on a treadmill, but may trigger Squat classification. In fact, if we train the network containing only the 7 exercises, we do not see this misclassification. As Fig. 7 shows, Bench Press when sensor on wrist is able to generate obvious body potential variation, but when sensor is attached on calf, the noise will cover the useful signals, this also explains the classification result of Bench Press with sensor on wrist and calf. Sensor with position in Pocket shows a more disordered classification than the other two sensor positions, because of the loosely coupled strength between body and circuit local ground as well as the friction between textile and sensor housing.

In general, classification is adequate in unseen subjects when the sensor is attached to the body on the calf or wrist. While reliable activity recognition was only achieved in the Walking and Running classes for sensors in the pocket, as we will discuss in section VI, this modality can still be used for workout counting.

VI. Evaluating Gym Workout Counting

A possible application scenario for the sensor is counting the repetitions of workout activities. In order to evaluate counting by itself, we performed counting exploration directly in the session's data, without first segmenting it using the classification pipeline. We did this in order to provide an upper bound to the possible counting accuracy. The real repetition times of each activity was recorded during all exercise(for Walking, steps were only recorded when walking on treadmills).

A. Counting Method

To evaluate the capabilities of the sensor for this case, we implemented a peak detector based counting method and applied it to all activity sessions.

The first step is using Fourier Transform to smooth the data. This approach is based on the principle of removing the higher order terms of the Fourier Transform of the signal, and so obtaining a smoothed function. Firstly, moving the signal in an activity window to the frequency domain (Fourier transform), then the undesired frequencies are removed, at last, signal is returned to the time domain(inverse fourier transform). This is implemented by using the package of fftpack from SciPy [26] Python library. Since differentiating between running and walking and the other five workouts works reasonably in all sensor placements, as depicted in Fig. 9 and Fig. 10, we use different parameters in our fourier transform based data smoothing method, that is, we filter different frequencies for Walking / Running and the other activities, since those two categories have different motion frequencies.

$$Accuracy = 1.0 - \frac{|count_{detected} - count_{real}|}{count_{real}} \quad (11)$$

The second step is detecting the peaks of the smoothed signal using the PeakUtils [27] python package. It works by, first, removing the undesired baseline, which is implemented by a function for estimating the baseline by using an iterative polynomial regression algorithm. Then peaks are detected

TABLE II
MACRO F-MEASURE RESULTS FOR OUR LEAVE ONE USER OUT PROCEDURE

	Sensor on Calf	Sensor in Pocket	Sensor on Wrist
One label per window	0.575 ± 0.03	0.486 ± 0.038	0.638 ± 0.068
One label per workout	0.569 ± 0.04	0.458 ± 0.05	0.639 ± 0.07

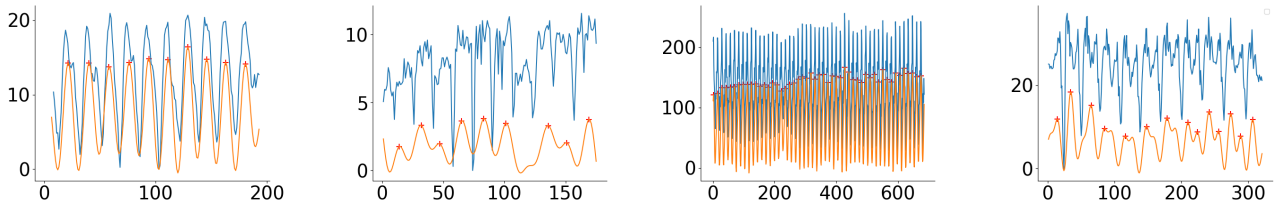

(a) L, Adductor, Fifth Day, Wrist, Repetition: 10, Detected: 10

(b) L, Bench Press, Second Day, Wrist, Repetition: 10, Detected: 9

(c) L, Walking, Fifth Day, Wrist, Repetition: 50, Detected: 50

(d) D, Leg Press, Fourth Day, Wrist, Repetition: 10, Detected: 14

Fig. 11: Workouts counting(X axis: sampled number(12Hz), Y axis:relative amplitude(uV), Blue line: original signal, orange line: smoothed signal, red $'+'$: detected peaks)

using the first and second order differences. To identify peaks correctly, two parameters are set: one is the threshold with relation to the highest value, another is minimum distance between two peaks. Here we set the first parameter as 0.3, second parameter for running and walking is 4 and for other workouts is 9(determined by the motion frequency, sample frequency is 12 Hz). Fig. 11 shows example of peak detection from the original data.

B. Counting Result

12 shows the distribution of counting accuracy for each workout type from each subject in all days, when sensor is located at the three positions. Accuracy is calculated by the formula 11. Step counting is widely used in daily life. Meredith [17] evaluated the accuracy of step counting based on smartphone applications and wearable devices, and got errors from -22.7% to 1.5% for the wearable devices, and 6.7% to 6.2% for smartphone applications. Unlike those inertial measurement unit based approaches, our capacitive coupling based sensor achieved counting accuracy with around 91%, which is highly competitive with devices on the market. As Fig. 12 depicted, the sensor worn on wrist has the best counting accuracy, and sensor in pocket also shows a satisfying accuracy, which demonstrates the feasibility of our sensor for non-contact counting. In all sensor positions, the activity of Bench Press shows the worst counting accuracy, which is as expected and reasonable, because of the small motion scale of body, as explained before. Another reason for a worse counting accuracy is the fake peaks detection, as showed by Fig. 11-d, in which the noisy signals will form fake peaks, which were not filtered out by the FFT smoothing. The best accuracy is achieved for Walking and Running, where there is an obvious distance change between ground and feet. Squat also shows a stable and high count accuracy, because of the big movement scale of the body related to ground. Fig. 13 presented the distribution of counting accuracy related to wearing configuration. As Table I listed, four types of wearing were employed. On the first and second day, all participants are dressed with polyester clothes, PVC shoes, and the shoes height is M, on the following three days we change the wearing configuration, this arrangement aims to explore the our recognition and counting accuracy influence from non-wearing and wearing factors. From Fig. 13 we can see that the counting accuracy of workouts, with the exception of Bench Press, is steadily located between 0.8 and 1.0 in each sensor position, without much deviation between the same or different user configurations, demonstrating that workout counting using our body capacitance-based sensor is feasible for most workouts.

VII. CONCLUSION AND FUTURE WORK

In this paper, we described an ultra-low power, capacitive coupling based sensor for full body gym workout counting and recognition. We evaluated it on 7 widely trained workouts in 3 body locations. The feasibility of our sensor was demonstrated by 15 segments of each workout activity with each sensor configuration from each of the 11 subjects. Our study showed promising results in workout counting with an average accuracy of 91% and leave one user out workout recognition of 63%, 56%, 45% for each sensor location regardless of individual wearing differences and weather conditions.

In general, *HBC* is a somewhat elusive concept, as the capacitance for each human body is not identical [21], it varies with different body postures (static standing or dynamic moving) [4], different garments (especially different shoes) [5], different body conditions(skin moisture, etc) [28], [29] as well as individual movement scale and speed. As a result, for activity recognition, many uncertain factors could hurt performance.

Future work will address this limitation by exploring the factors that will influence body potential variation. As we have already recorded different user configurations, in future work we will perform a deeper analysis of the influence of those factors on the signal. Besides that, we will work on improving the counting procedure (for example, overcoming the fake peak detection, etc) as well as the activity recognition

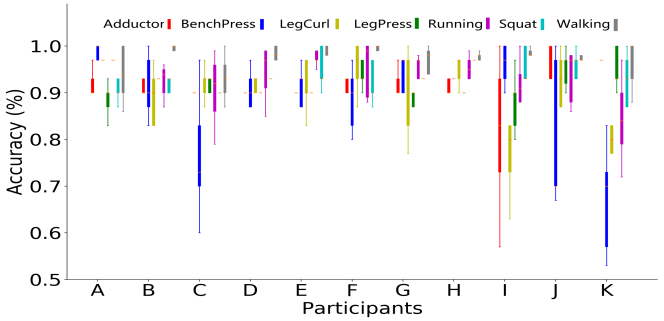

(a) Workouts counting accuracy of each Participant with sensor on calf, overall: (0.916±0.080)%

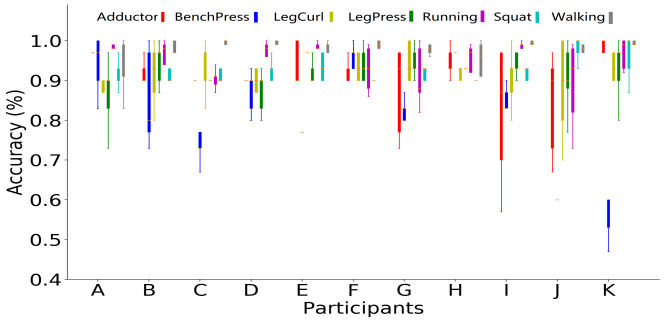

(b) Workouts counting accuracy of each Participant with sensor on Wrist, overall: (0.910±0.098)%

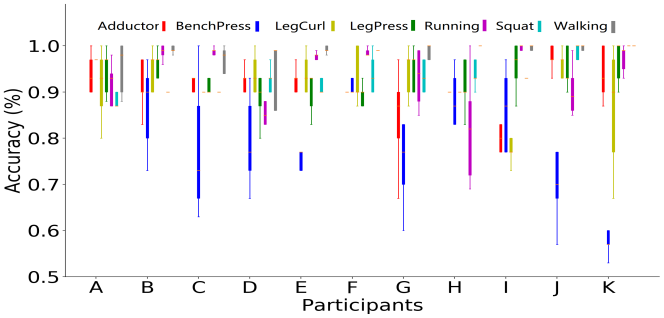

(c) Workouts counting accuracy of each Participant with sensor in Pocket, overall: (0.913±0.091)%

Fig. 12: Accuracy of workouts counting for each participant in all days with different sensor location (overall accuracy is calculated regardless of participants, workouts type and date)

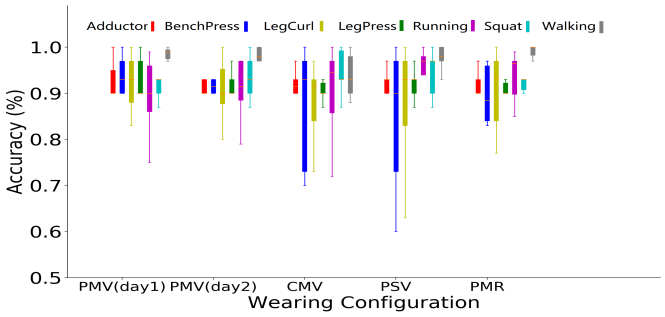

(a) Workouts counting accuracy of different wearing configuration with sensor on calf

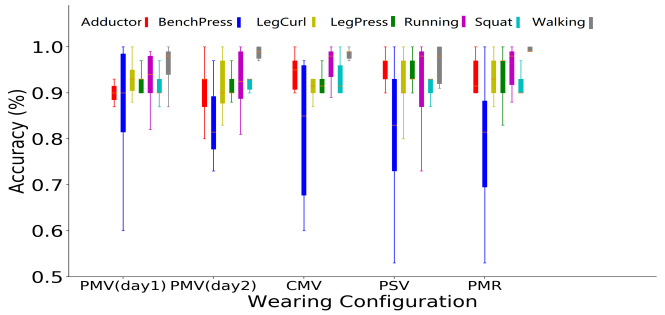

(b) Workouts counting accuracy of different wearing configuration with sensor on Wrist

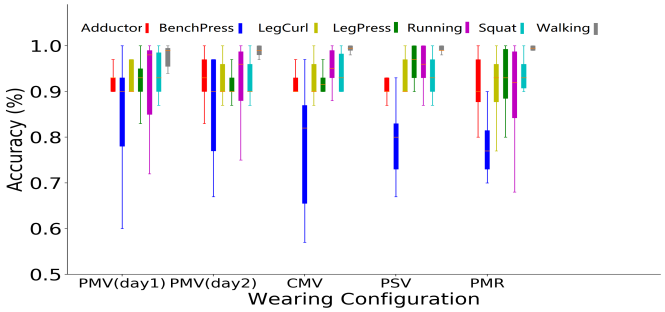

(c) Workouts counting accuracy of different wearing configuration with sensor in Pocket

Fig. 13: Accuracy of workouts counting of different wearing configuration by all participants with different sensor location(Wearing Configuration P:Polyester, C:Cotton, M,S:sole height, V:PVC, R;Rubber)

procedure and their integration, so that at last the system can be used to seamlessly recognize and count gym activities during a whole gym session.

ACKNOWLEDGMENT

The work was funded by the German Federal Ministry of Education and Research (BMBF) through the project iGroups (grant nr. 01IW15004).

REFERENCES

[1] J. R. Kwapisz, G. M. Weiss, and S. A. Moore, "Activity recognition using cell phone accelerometers," *ACM SigKDD Explorations Newsletter*, vol. 12, no. 2, pp. 74–82, 2011.

[2] E. Mitchell, D. Monaghan, and N. E. O'Connor, "Classification of sporting activities using smartphone accelerometers," *Sensors*, vol. 13, no. 4, pp. 5317–5337, 2013.

[3] A. K. A. B. Biying Fu, Florian Kirchbuchner and D. V. Gangatharan, "Fitness activity recognition on smartphones using doppler measurements," *Informatics*, 2018.

[4] N. Jonassen, "Human body capacitance: static or dynamic concept?[esd]," in *Electrical Overstress/Electrostatic Discharge Symposium Proceedings, 1998*. IEEE, 1998, pp. 111–117.

[5] O. Fujiwara and T. Ikawa, "Numerical calculation of human-body capacitance by surface charge method," *Electronics and Communications in Japan (Part I: Communications)*, vol. 85, no. 12, pp. 38–44, 2002.

[6] T. G. Zimmerman, J. R. Smith, J. A. Paradiso, D. Allport, and N. Gershenfeld, "Applying electric field sensing to human-computer interfaces," in *Proceedings of the SIGCHI conference on Human factors in computing systems*. ACM Press/Addison-Wesley Publishing Co., 1995, pp. 280–287.

[7] M. Hirsch, J. Cheng, A. Reiss, M. Sundholm, P. Lukowicz, and O. Amft, "Hands-free gesture control with a capacitive textile neckband," in *Proceedings of the 2014 ACM International Symposium on Wearable Computers*. ACM, 2014, pp. 55–58.

[8] G. Cohn, D. Morris, S. Patel, and D. Tan, "Humantenna: using the body as an antenna for real-time whole-body interaction," in *Proceedings*

of the SIGCHI Conference on Human Factors in Computing Systems. ACM, 2012, pp. 1901–1910.

[9] P. G. Hallenberg and E. Hove, "System and method for communicating through a capacitive touch sensor," Sep. 6 2016, uS Patent 9,436,322.

[10] M. Sato, I. Poupyrev, and C. Harrison, "Touché: enhancing touch interaction on humans, screens, liquids, and everyday objects," in *Proceedings of the SIGCHI Conference on Human Factors in Computing Systems*. ACM, 2012, pp. 483–492.

[11] J. Cheng, O. Amft, and P. Lukowicz, "Active capacitive sensing: Exploring a new wearable sensing modality for activity recognition," in *International Conference on Pervasive Computing*. Springer, 2010, pp. 319–336.

[12] G. Cohn, S. Gupta, T.-J. Lee, D. Morris, J. R. Smith, M. S. Reynolds, D. S. Tan, and S. N. Patel, "An ultra-low-power human body motion sensor using static electric field sensing," in *Proceedings of the 2012 ACM Conference on Ubiquitous Computing*. ACM, 2012, pp. 99–102.

[13] A. Pouryazdan, R. J. Prance, H. Prance, and D. Roggen, "Wearable electric potential sensing: a new modality sensing hair touch and restless leg movement," in *Proceedings of the 2016 ACM International Joint Conference on Pervasive and Ubiquitous Computing: Adjunct*. ACM, 2016, pp. 846–850.

[14] J. von Wilmsdorff, F. Kirchbuchner, B. Fu, A. Braun, and A. Kuijper, "An exploratory study on electric field sensing," in *European Conference on Ambient Intelligence*. Springer, 2017, pp. 247–262.

[15] C. Harland, T. Clark, and R. Prance, "Electric potential probes-new directions in the remote sensing of the human body," *Measurement Science and technology*, vol. 13, no. 2, p. 163, 2001.

[16] K. Kurita, R. Takizawa, and H. Kumon, "Detection of human walking motion based on measurement system of current generated byelectrostatic induction," 2009.

[17] M. A. Case, H. A. Burwick, K. G. Volpp, and M. S. Patel, "Accuracy of smartphone applications and wearable devices for tracking physical activity data," *Jama*, vol. 313, no. 6, pp. 625–626, 2015.

[18] E. Terzic, J. Terzic, R. Nagarajah, and M. Alamgir, "Capacitive sensing technology," in *A Neural Network Approach to Fluid Quantity Measurement in Dynamic Environments*. Springer, 2012, pp. 11–37.

[19] G. Castle, "Contact charging between insulators," *Journal of Electrostatics*, vol. 40, pp. 13–20, 1997.

[20] T. Grosse-Puppendahl, X. Dellangnol, C. Hatzfeld, B. Fu, M. Kupnik, A. Kuijper, M. R. Hastall, J. Scott, and M. Gruteser, "Platypus: Indoor localization and identification through sensing of electric potential changes in human bodies," in *Proceedings of the 14th Annual International Conference on Mobile Systems, Applications, and Services*. ACM, 2016, pp. 17–30.

[21] R. M. Fish and L. A. Geddes, "Conduction of electrical current to and through the human body: a review," *Eplasty*, vol. 9, 2009.

[22] S. Bai, J. Z. Kolter, and V. Koltun, "An empirical evaluation of generic convolutional and recurrent networks for sequence modeling," *arXiv preprint arXiv:1803.01271*, 2018.

[23] F. Chollet *et al.*, "Keras," https://keras.io, 2015.

[24] M. Abadi, A. Agarwal, P. Barham, E. Brevdo, Z. Chen, C. Citro, G. S. Corrado, A. Davis, J. Dean, M. Devin, S. Ghemawat, I. Goodfellow, A. Harp, G. Irving, M. Isard, Y. Jia, R. Jozefowicz, L. Kaiser, M. Kudlur, J. Levenberg, D. Mané, R. Monga, S. Moore, D. Murray, C. Olah, M. Schuster, J. Shlens, B. Steiner, I. Sutskever, K. Talwar, P. Tucker, V. Vanhoucke, V. Vasudevan, F. Viégas, O. Vinyals, P. Warden, M. Wattenberg, M. Wicke, Y. Yu, and X. Zheng, "TensorFlow: Large-scale machine learning on heterogeneous systems," 2015, software available from tensorflow.org. [Online]. Available: https://www.tensorflow.org/

[25] D. P. Kingma and J. Ba, "Adam: A method for stochastic optimization," *CoRR*, vol. abs/1412.6980, 2014. [Online]. Available: http://arxiv.org/abs/1412.6980

[26] E. Jones, T. Oliphant, P. Peterson *et al.*, "SciPy: Open source scientific tools for Python," 2001–, [Online; accessed 2018-05-16]. [Online]. Available: http://www.scipy.org/

[27] L. H. Negri, "PeakUtils: Open source scientific tools for Python," 2014–, [Online; accessed 2018-09-10]. [Online]. Available: https://peakutils.readthedocs.io/en/latest/peakutils

[28] N. Goad and D. Gawkrodger, "Ambient humidity and the skin: The impact of air humidity in healthy and diseased states," *Journal of the European Academy of Dermatology and Venereology*, vol. 30, no. 8, pp. 1285–1294, 2016.

[29] M. Egawa, M. Oguri, T. Kuwahara, and M. Takahashi, "Effect of exposure of human skin to a dry environment," *Skin Research and Technology*, vol. 8, no. 4, pp. 212–218, 2002.